K. SOBCZYK*, J. ZBROSZCZYK*, M. NABIAŁEK*, J. OLSZEWSKI*, P. BRĄGIEL** J. ŚWIERCZEK* W. CIURZYŃSKA*, A. ŁUKIEWSKA*, M. LUBAS***, M. SZOTA***

MICROSTRUCTURE, MAGNETIC PROPERTIES AND CRYSTALIZATION BEHAVIOUR OF BULK AMORPHOUS $Fe_{61}Co_{10}Zr_{2.5}Hf_{2.5}Ni_2W_2B_{20}$ ALLOY

MIKROSTRUKTURA, WŁAŚCIWOŚCI MAGNETYCZNE I KRYSTALIZACJA MASYWNEGO STOPU AMORFICZNEGO $Fe_{61}Co_{10}Zr_{2.5}Hf_{2.5}Ni_2W_2B_{20}$

Microstructure by X-ray diffractometry and Mö ssbauer spectroscopy and some magnetic properties such as magnetic polarization curves, magnetic permeability, total core losses and approach to magnetic saturation for the bulk amorphous $Fe_{61}Co_{10}Zr_{2.5}Hf_{2.5}Ni_2W_2B_{20}$ alloy in the as-quenched state and after heat treatment at 850 K for 15 min are studied. The as-cast samples in the form of plates are fully amorphous and after annealing the samples are partially crystallized. The grains of $Fe_{80}Co_{20}$ and disordered Fe_3B phases with the volume fraction each of 0.05 are embedded in the amorphous matrix which is much more inhomogeneous than in the as-quenched state. The maximum magnetic permeability measured at 50 Hz and the magnetic saturation polarization increase from 1700 and 1.25 T in the as-cast state to 1800 and 1.47 T after heat treatment, respectively. The rotation of magnetic moments in the vicinity of point-like defects plays the decisive role in approach to ferromagnetic saturation in the as-quenched sample, whereas in the annealed sample the rotation of magnetic moments near the quasi-dislocation dipoles seems to be dominant. It indicates that during annealing the agglomeration of point-like defects takes place.
Keywords: bulk amorphous alloys, Mössbauer spectroscopy, magnetic permeability, total core losses and approach to ferromagnetic saturation

Badano mikrostrukturę, wykorzystując dyfrakcję promieniowania X oraz spektroskopię mössbauerowską oraz niektóre własciwości magnetyczne, takie jak: polaryzację magnetyczną przenikalność, straty całkowite na przemagnesowanie oraz podejście do ferromagnetycznego nasycenia dla masywnego stopu $Fe_{61}Co_{10}Zr_{2.5}Hf_{2.5}Ni_2W_2B_{20}$ w stanie po zestaleniu i po obróbce cieplnej w 850 K przez 15 min. Próbki w kształcie płytek w stganie po zestaleniu są amorficzne, natomiast po wygrzaniu są częściowo skrystalizowane. Ziarna fazy $Fe_{80}Co_{20}$ i nieuporządkowanej Fe_3B o ułamku objętościowym 0.05 są umieszczone w matrycy amorficznej, która jest bardziej niejednorodna niż w stanie po zestaleniu.

Maksymalna przenikalność magnetyczna mierzona przy częstości pola magnesującego 50 Hz i wartość magnetycznej polaryzacji nasycenia wzrastają odpowiednio z 1700 i 1.25 T w stanie po zestaleniu do 1800 oraz 1.47 T po obróbce cieplnej.

Proces magnesowania w pobliżu ferromagnetycznego nasycenia w próbce po zestaleniu zachodzi głównie poprzez obrót momentów magnetycznych w pobliżu defektów punktowych, natomiast w próbce poddanej obróbce cieplnej – poprzez obroty momentów magnetycznych w pobliżu pseudo – dyslokacyjnych dipoli. Podczs wygrzewania próbki następuje aglomeracja defektów punktiwych i tworzą się pseudo-dyslokacyjne dipole.

1. Introduction

Preparation of classical amorphous alloys in the form of ribbons with the thickness smaller than 50 μm requires high cooling rates of order of 10^5 K/s [1, 2]. This limits the application of these materials in industry. Multicomponent systems of elements with large differences in atomic radii exhibit high glass forming ability and can be obtained in the amorphous state not only in ribbon form but like plates, rods and tubes, and are known as bulk amorphous materials [3, 4]. These alloys are usually obtained at much lower quenching rate (1 - 10^2) K/s. So, the bulk amorphous materials are partially stress – relieved during preparation and smaller

* INSTITUTE OF PHYSICS, CZĘSTOCHOWA UNIVERSITY OF TECHNOLOGY, ARMII KRAJOWEJ AV. 19, 42-200 CZĘSTOCHOWA, POLAND
** INSTITUTE OF PHYSICS, CZĘSTOCHOWA UNIVERSITY OF TECHNOLOGY, ARMII KRAJOWEJ AV. 19, 42-200 CZĘSTOCHOWA, POLAND
*** INSTITUTE OF ENGINEERING MATERIALS, CZĘSTOCHOWA UNIVERSITY OF TECHNOLOGY, ARMII KRAJOWEJ AV. 19, 42-200 CZĘSTOCHOWA, POLAND

density of structure defects and high stability of physical properties should be expected. The bulk amorphous alloys crystallize usually at one stage at the temperature depending on both their chemical composition and the form of samples. Iron-based bulk amorphous alloys are especially attractive because of their small coercivity, relatively high magnetic saturation polarization and low core losses.

In this paper we present the microstructure, magnetic properties i.e. permeability, core losses and approach to ferromagnetic saturation studies for the bulk amorphous and partially crystallized $Fe_{61}Co_{10}Zr_{2.5}Hf_{2.5}Ni_2W_2B_{20}$ alloy.

2. Experimental procedure

Ingots of the alloy were prepared by arc melting of high purity elements in an argon atmosphere. The bulk amorphous $Fe_{61}Co_{10}Zr_{2.5}Hf_{2.5}Ni_2W_2B_{20}$ alloy was obtained in the form of plates 0.5 mm thick by the suction casting method [5]. The amorphicity of the samples was checked by X-ray diffractometry and Mössbauer spectroscopy. Mössbauer spectra in a transmission geometry were recorded by a conventional spectrometer working at constant acceleration with $^{57}Co(Rh)$ radioactive source of 50 mCi activity. Mössbauer spectroscopy was also applied to analyze the microstructure of the partially crystallized samples subjected to the annealing at 850 K for 15 min. The annealing temperature was determined from DSC (differential scanning calorimetry) curves recorded at the heating rate of 10K/min [6].

The magnetic permeability and core losses of the samples in the as-quenched state and after annealing were measured by a transformer method using a completely automated set-up. The magnetic polarization, $\mu_0 M$, as a function of the magnetizing field induction, B, was measured by a vibrating sample magnetometer (VSM). From $\mu_0 M(B)$ curves measured in high magnetic fields, where the domain structure is not present in the sample, the approach to magnetic saturation was analyzed.

3. Results and discussion

In Fig. 1 the X-ray diffraction pattern for the as-quenched sample of the bulk $Fe_{61}Co_{10}Zr_{2.5}Hf_{2.5}Ni_2W_2B_{20}$ alloy is shown. It can be seen that only one broad maximum characteristic of fully amorphous materials is present.

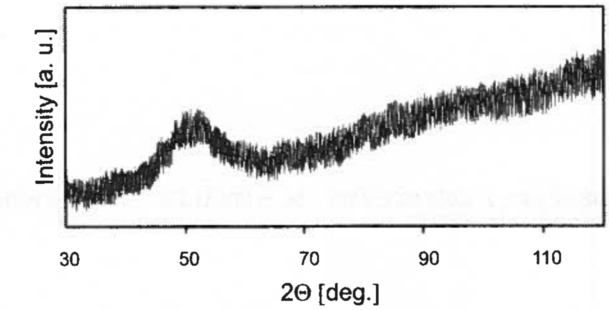

Fig. 1. X-ray diffraction pattern for the as-cast $Fe_{61}cO_{10}zR_{2.5}hF_{2.5}nI_2w_2b_{20}$ alloy

The Mössbauer spectrum and corresponding hyperfine magnetic field distribution for the as-received sample are depicted in Fig. 2a. The spectrum consists of broad and overlapping lines typical for the amorphous ferromagnets. The hyperfine field distribution obtained from this spectrum has a log-normal form and may be presented as a linear combination of Gaussian distributions indicating that this alloy is relatively homogeneous (Fig. 2b).

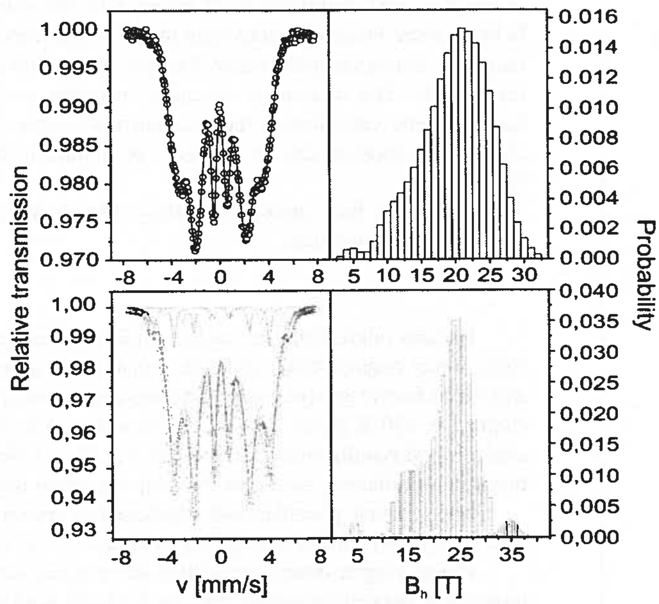

Fig. 2. Transmission Mössbauer spectra (a, c) and corresponding hyperfine field distributions (b, d) for the bulk amorhous $Fe_{61}cO_{10}zR_{2.5}hF_{2.5}nI_2w_2b_{20}$ alloy in the as-quenched state (a, b) and after annealing at 850 K for 15 min. (c, d)

Fig. 3 shows the DSC curve for the as-quenched $Fe_{61}cO_{10}zR_{2.5}hF_{2.5}nI_2w_2b_{20}$ alloy obtained at the heating rate of 10 K/min. In the curve only one exothermic peak at 855 K is visible indicating that this alloy crystallizes in one stage. The onset of the crystallization is observed at 845 K (Fig. 3). The half width of the exothermic peak is about 10 K which confirms that the crystallization process is complex and takes place at the narrow range of temperature.

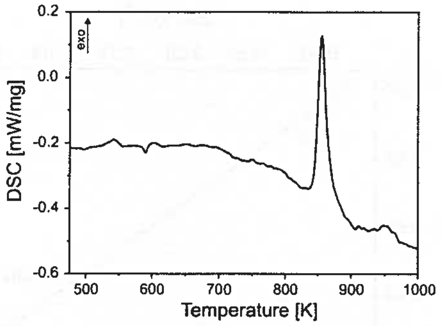

Fig. 3. DSC curves for the bulk amorphous $Fe_{61}cO_{10}zR_{2.5}hF_{2.5}nI_2w_2b_{20}$ alloy obtained at the heating rate of 10 K/min

The Mössbauer spectrum of the sample annealed at 850 K for 15 min is presented in Fig. 2c. In this spectrum three different components can be distinguished. The hyperfine field parameters obtained from Mössbauer spectra analysis are listed in Table I. Two subspectra correspond to two crystalline phases: one of them is connected with α-FeCo phase with Co concentration of about 20 at %. and the volume fraction of 0.05, the second one is ascribed to the disordered Fe_3B phase with the volume fraction of 0.05. The third main component is connected with the residual amorphous matrix. From the hyperfine field distribution (Fig. 2d) is seen that the amorphous matrix is highly inhomogeneous.

TABLE 1

The average values of the hyperfine megnetic field induction in amorphous phases (B_{effam}) thier standard deviations (ΔB_{effam}) the hyperfine magnetic field induction of the crystalline phases (B_{cr}) and thier volume fraction (V_{cr}) for the bulk amorphous $Fe_{61}cO_{10}zR_{2.5}hF_{2.5}nI_2w_2b_{20}$ alloy in the asquenched state and after the heat treatment at 850K for 15 min.

thermal history of the sample	B_{effam} [T]	ΔB_{effam} [T]	phase	B_{cr} [T]	V_{cr}
as-quenched	19,91	5.11	–	–	–
annealin at 850 K for 15 min	22.31	5.20	$Fe_{80}Co_{20}$	34.68	0.05
			disordered Fe_3B	24.37	0.05

In Fig. 4 the magnetic polarization curves $\mu_0M(H)$ for the sample of the $Fe_{61}cO_{10}zR_{2.5}hF_{2.5}nI_2w_2b_{20}$ alloy in the as-quenched state and after annealing at 850 K for 15 min are shown. A distinct increase of the magnetic saturation polarization from 1.25 T to 1.47 T after the heat treatment of the sample is observed. It is connected with the appearance of ? FeCo and FeB crystalline phases.

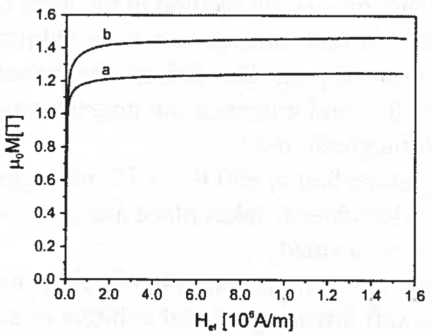

Fig. 4. The magnetic polarization, μ_0M, versus the effective magnetizing field, H_{ef} for $Fe_{61}cO_{10}zR_{2.5}hF_{2.5}nI_2w_2b_{20}$ alloy in the as-quenched state (a) and after annealing at 850 K for 15 min (b)

The magnetic permeability versus the amplitude of the magnetizing field, measured at two different frequencies for the as-quenched and annealed samples is depicted in Fig. 5. The maximum permeability for the as received sample at the frequency of 50 Hz is equal to 1700 and after annealing at 850 K for 15 min a slight increase of its value to 1800 is observed. This also confirms that the fine crystalline grains in the annealed samples are present [7].

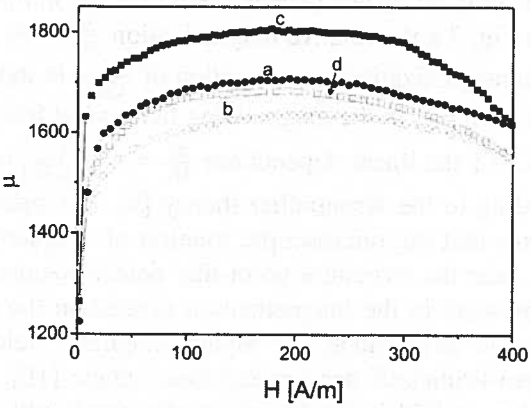

Fig. 5. The magnetic permeability, μ, versus the amplitude of the magnetizing field with two different frequencies: 50 Hz (a, c) and 1000 Hz (b, d) for $Fe_{61}cO_{10}zR_{2.5}hF_{2.5}nI_2w_2b_{20}$ alloy in the as-quenched state (a, b) and after annealing at 850 K for 15 min (c, d)

Total core losses, P, versus the amplitude of the magnetizing field induction for four different frequencies are presented in Fig. 6a. The value of P in the as-cast bulk amorphous $Fe_{61}cO_{10}zR_{2.5}hF_{2.5}nI_2w_2b_{20}$ alloy at the amplitude of the magnetizing field induction of 0.2 T and at the frequency of 50 Hz is about $4\frac{W}{kg}$ and is nearly ten times smaller than in the classical non-magnetostrictive amorphous $Co_{70.5}Fe_{4.5}Si_{10}B_{15}$ ribbon [8]. After annealing at 850 K for 15 min no distinct changes of core losses are observed (Fig. 6b).

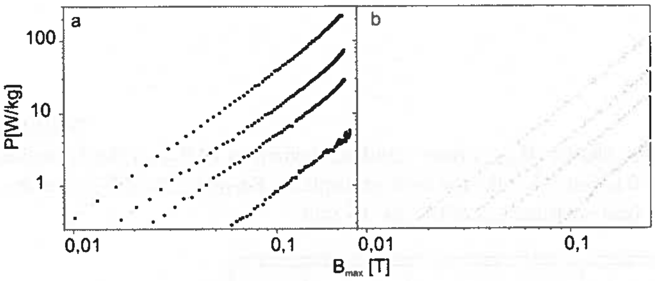

Fig. 6. The total core losses, P, versus the amplitude of the magnetizing field induction, B, for the bulk amorphous $Fe_{61}cO_{10}zR_{2.5}hF_{2.5}nI_2w_2b_{20}$ alloy in the as-quenched state (a) and after annealing at 850 K for 15 min (b)

Because of the lower quenching rate during preparation of the bulk amorphous $Fe_{61}cO_{10}zR_{2.5}hF_{2.5}nI_2w_2b_{20}$ alloy in the form of a plate than for classical amorphous ribbons only point-like defects seem to occur in the sample. In Fig. 7 a the relative magnetization $\frac{M}{M_S}$ (M_S – saturation magnetization) as a function of $\frac{1}{\sqrt{\mu_0 H}}$ is shown. It can be seen that in the magnetizing field range from 0.15 T to 0.30 T the linear dependence $\frac{M}{M_S} = f\left(\frac{1}{\sqrt{\mu_0 H}}\right)$ occurs. According to the Kronmüller theory [9], this behaviour confirms that the microscopic rotation of magnetic moments near the structural point-like defects seems to be the dominant in the magnetization process in the above mentioned field range. At higher magnetic fields the Holstein-Primakoff paraprocess takes place [10]. After annealing at 850 K for 15 min in the comparable magnetizing field range the linear dependence $\frac{M}{M_S} = f\left(\frac{1}{\mu_0 H}\right)$ occurs (Fig. 7 b). The observed effect indicates that the rotation of magnetic moments near the quasi - dislocation dipoles plays the main role in the magnetization process. During annealing the thermal activated diffusion of atoms leads to agglomeration of point-like defects and linear ones called the quasi – dislocation dipoles are created.

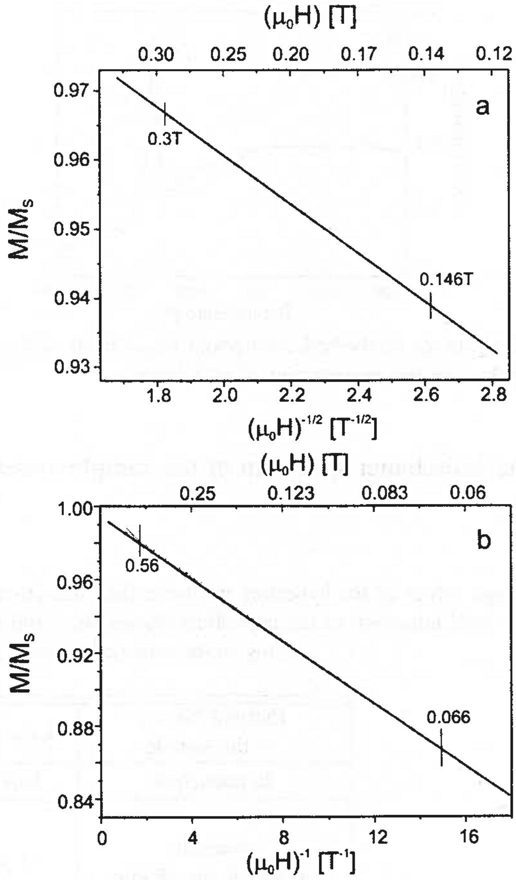

Fig. 7. The relative magnetization M/M_S versus $1/\sqrt{\mu_0 H}$ for $Fe_{61}cO_{10}zR_{2.5}hF_{2.5}nI_2w_2b_{20}$ alloy in the as-quenched state (a) and M/M_S versus $1/\mu_0 H$ for $Fe_{61}cO_{10}zR_{2.5}hF_{2.5}nI_2w_2b_{20}$ alloy after annealing at 850 K 15 min (b)

4. Conclusions

- The bulk $Fe_{61}cO_{10}zR_{2.5}hF_{2.5}nI_2w_2b_{20}$ alloy obtained by the suction-casting method in the form of plate 0.5 mm thick is fully amorphous. Free volumes, mainly in the form of point-like defects are presented in the as-cast alloy and influence the magnetization process in high magnetic fields.
- During annealing at 850 K for 15 min agglomeration of point-like defects takes place and quasi-dislocation dipoles are formed.
- The bulk amorphous $Fe_{61}cO_{10}zR_{2.5}hF_{2.5}nI_2w_2b_{20}$ alloy is a soft ferromagnet and exhibits relatively large maximum permeability and low total core losses.
- During crystallization of this alloy fine grains of two crystalline phases (α-FeCo and Fe_2B) appear.
- The magnetic saturation polarization increases from 1.25 T in the as-quenched state to 1.47 T after heat treatment at 850 K for 15 min. Simultaneously the enhancement of the maximum of magnetic permeability from 1700 to 1800 is observed.

REFERENCES

[1] P. I. Williams, A. J. Moses, T. Meydan, R. J. D. Tilley, Amorphization of bulk magnetic materials by an arc melting technique, J. Magn. Magn. Mater. 254-255, 17 (2003).

[2] . Hasegawa, Soft magnetic properties of metallic glasses, J. Magn. Magn. Mater. **41**, 79 (1984).

[3] A. Inoue, A. Makino, T. Mizushima, Ferromagnetic bulk glassy alloys, J. Magn. Magn. Mater., 215-216, 246 (2000).

[4] . Inoue, Bulk amorphous alloys: Preparation and fundamental characteristic, Mater. Sci. Fundations 6 (1998) Trans. Tech. Publications.

[5] P. Pawlik, M. Nabiałek, E. Żak, J. Zbroszczyk, J. J. Wysłocki, J. Olszewski, K. Pawlik, Processing of bulk amorphous alloys by suction-casting method, Arch. Mater. Sci. **25** (3), 177 (2004).

[6] M. Al-Haj, J. Barry, Nanocrystallization kinetics of $Fe_{85.5}Zr_4Nb_4B_{5.5}Al_1$ amorphous alloy, J. Mater. Sci. Lett. **17**, 1125 (1998).

[7] G. Herzer, Grain size dependence of coercivity and permeability in nanocrystalline ferromagnets, IEEE Trans. Magn. 26, 1397 (1990).

[8] A. Makino, T. Hatanai, A. Inoue, T. Masumoto, Nanocrystalline soft magnetic Fe-M-B (M=Zr, Hf, Nb) alloys and their applications, Mater. Sci. Eng. **A 226 - 228**, 594 (1997).

[9] H. Kronmüller, Magnetization processes and the microstructure in amorphous metals, J. de Phys. **41**, 518 (1980).

[10] T. Holstein, H. Primakoff, Magnetization near saturation in polycrystalline ferromagnets, Phys. Rev. 59, 388 (1941).

Received: 10 June 2008.